Supporting Information

ATP-Responsive ZIF-based NIR Fluorescent Nanosystem for Enhanced Chemo-Photodynamic Therapy of Tumors

Si-Si Chen,[a] Xiao-Fan Xu,[a] Wei-Qun Deng,[a] Liufang Hu,[a] Juan Ouyang,[a,*] Chun-Yan Li[a,*]

[a] Key Laboratory for Green Organic Synthesis and Application of Hunan Province, Key Laboratory of Environmentally Friendly Chemistry and Applications of Ministry of Education, College of Chemistry, Xiangtan University, Xiangtan, 411105, PR China.

[b] Henan Key Laboratory of Organic Functional Molecule and Drug Innovation, Collaborative Innovation Center of Henan Province for Green Manufacturing of Fine Chemicals, Key Laboratory of Green Chemical Media and Reactions, Ministry of Education, School of Chemistry and Chemical Engineering, Henan Normal University, Xinxiang, 453007, PR China.

*Corresponding Author. E-mail: oyj2023@xtu.edu.cn, lichunyan@xtu.edu.cn.

Table of contents

1 Experimental section

1.1 Reagents

Iodoethane, 3-bromopropylamine hydrobromide, 2,3,3-trimethylindolenine and adenosine 5’-triphosphate disodium (ATP) were purchased from Macklin (Shanghai, China). Cyclohexanone, phosphorus oxide trichloride, doxorubicin hydrochloride, imidazole-2-carboxaldehyde (2-ICA), zinc acetate dihydrate, 2',7'-Dichlorofluorescein (DCFH) and 2',7'-Dichlorofluorescein diacetate (DCFH-DA) were procured from Aladdin (Shanghai, China). Cell counting kit-8 (CCK-8), calcein AM/propidium (AM/PI) and assay buffer were obtained from Shanghai Beyotime Biotechnology Co., Ltd. Unless otherwise specified, all chemical reagents mentioned above were used directly without additional purification. Triple-distilled water was used throughout the experiments.

1.2 Apparatus

Nuclear magnetic resonance (NMR) spectra were measured on a Bruker Avance II NMR spectrometer (Germany). Mass spectra (MS) were recorded on a Bruker Autoflex MALDI-TOF mass spectrometer (Germany). Scanning electron microscope (SEM) images were captured utilizing a ZEISS sigma microscope. Powder X-ray diffraction patterns (PXRD) were performed by a Rigaku Mini flex600 X-ray diffraction (Japan). FT-IR spectra were recorded with Bruker Fourier transform infrared spectrometer. Thermogravimetric analysis (TGA) was conducted on a TGA-50 instrument (Japan). Transmission electron microscopy (TEM) images were examined by a FEI Talos S-FEG transmission electron microscopy (Germany). Absorption spectra were acquired using an Agilent CARY 60 UV-vis spectrophotometer (USA). Fluorescence spectra were collected on a Hitachi F-4600 spectrophotometer (Japan). Confocal laser scanning microscopy (CLSM) images were obtained using a Nikon confocal fluorescence microscope (Japan). Live and dead cell staining images were recorded with an Olympus FV3000 fluorescence microscope (Japan). Fluorescence imaging was performed using an IVIS Lumina XR small animal optical in vivo imaging system (USA).

1.3 Syntheses

Synthesis of compound 1-3. Compound 1-3 was synthesized according to the reported literature.[S1]

Synthesis of Cy. Compound 1 (1.89 g, 6.0 mmol) and compound 2 (1.00 g, 5.8 mmol) were dissolved in a mixture of solvents (1-butanol: benzene = 7:3, v/v) and stirred at 110 °C under a nitrogen atmosphere for 2 h. Subsequently, compound 3 (2.26 g, 6.0 mmol) was added to the reaction mixture and stirred at 120 °C while removing water for 12 h. The solvents were then removed under vacuum, and the resulting residue was washed with ether. The crude product was purified by silica gel chromatography with CH_2Cl_2/CH_3OH (25/1, v/v) as eluent to afford a green solid product. Yield: 2.5 g (70%). ^{1}H NMR (400 MHz, DMSO-d_6, Fig. S1) δ 8.31 (d, J = 14.4 Hz, 1H), 8.17 (d, J = 13.8 Hz, 1H), 7.67 (d, J = 8.0 Hz, 1H), 7.58 (d, J = 7.4 Hz, 1H), 7.53 (d, J = 7.9 Hz, 1H), 7.45 (t, J = 7.7 Hz, 1H), 7.40 (t, J = 5.4 Hz, 1H), 7.33 (t, J = 7.4 Hz, 1H), 7.22 (t, J = 7.9 Hz, 1H), 6.43 (d, J = 14.4 Hz, 1H), 6.20 (d, J = 14.0 Hz, 1H), 4.31 (d, J = 7.1 Hz, 2H), 4.23 (t, J = 8.0 Hz, 2H), 2.93 (t, J = 7.8 Hz, 2H), 2.71 (d, J = 6.3 Hz, 4H), 1.97 (t, J = 7.8 Hz, 2H), 1.83 (t, J = 8.0 Hz, 2H), 1.66 (s, 6H), 1.65 (s, 6H), 1.30 (t, J = 7.1 Hz, 3H). ^{13}C NMR (101 MHz, DMSO-d_6, Fig. S2) δ 174.07, 171.05, 148.52, 145.13, 142.64, 142.12, 142.06, 141.88, 141.11, 129.28, 128.98, 127.21, 126.49, 126.43, 125.00, 123.19, 123.04, 112.54, 111.19, 103.60, 100.44, 56.50, 50.04, 49.04, 41.15, 37.08, 28.14, 27.72, 26.45, 25.58, 20.87, 19.03, 12.96. MALDI-TOF-MS (ESI) (m/z, Fig. S3): calcd. 540.314, found 540.406.

Synthesis of ZIF-90 nanoparticles. ZIF-90 was synthesized according to the reported literature.[S2]

Synthesis of DZ nanoparticles. DZ was synthesized according to the reported literature.[S3]

Synthesis of CZ nanosystem. A DMF solution (2 mL) of zinc acetate dihydrate (0.2 M) was poured into a DMF solution (2 mL) of 2-ICA (0.2 M) containing Cy (2 mg) under vigorous stirring at room temperature. After 5 min, DMF (6 mL) was added into the

reaction mixture to stabilize the structure. The resulting nanoparticles were then purified by centrifugation (10000 rpm, 5 min) and washed with DMF once and ethanol in turn for several times. The nanoparticles were then collected and dried under vacuum at room temperature for 24 h.

Synthesis of CDZ nanosystem. A DMF solution (2 mL) of zinc acetate dihydrate (0.2 M) was poured into a DMF solution (2 mL) of 2-ICA (0.2 M) containing Cy (2 mg) and DOX (2 mg) under vigorous stirring at room temperature. After 5 min, DMF (6 mL) was added into the reaction mixture to stabilize the structure. The resulting nanoparticles were then purified by centrifugation (10000 rpm, 5 min) and washed with DMF once and ethanol in turn for several times. The nanoparticles were then collected and dried under vacuum at room temperature for 24 h.

1.4 Optical response of the nanosystem toward ATP

Various concentrations of ATP were added into a solution of CDZ (final CDZ concentration: 4 mg/mL, ATP concentration: 0-10 mM, in HEPES buffer solution (10 mM, pH = 7.4, 5% DMSO)). Subsequently, the reaction solutions were incubated at 37 °C for 0-30 min, and their absorption and fluorescence spectra were assessed. Fluorescence spectra were recorded with the excitation at 770 nm and the emission at 780-900 nm. Both the excitation and emission slits were set to 5 nm.

1.5 Encapsulation, loading and release profiles of DOX from CDZ

For the encapsulation efficiency and loading efficiency of DOX, according to the synthesis of CDZ nanosystem, the amount of unloaded DOX was determined by measuring the absorbance at 480 nm of supernatant with UV-vis spectrophotometer and comparing it with the DOX standard curve. Furthermore, the following two formulas were utilized to calculate encapsulation efficiency and loading efficiency:

$$\text{Encapsulation efficiency\%} = \frac{m_0 - m_1}{m_0} \times 100\%$$

$$\text{Loading efficiency\%} = \frac{m_0 - m_1}{m_2} \times 100\%$$

where m_0 is the amount of initial DOX, m_1 is the amount of unloaded DOX, m_2 is the amount of CDZ. The encapsulation efficiency and loading efficiency of DOX in CDZ were determined as 69 wt% and 3.45 wt%, respectively.

In vitro drug release profile of DOX from the CDZ nanosystem was evaluated in PBS (pH 7.4, containing 10% DMSO. CDZ nanosystem (3.75 mL) was added into a dialysis bag (with a molecular weight cut-off of 1000 Da), and then immersed into the release medium (50 mL, 10 mM ATP in PBS solution (pH 7.4)) which was incubated in a shaking water bath with 100 rpm at 37 ℃. At the designated time intervals, the aliquots (2 mL) were taken out and the release medium was replenished with fresh release medium to 50 mL. Through the absorption-based calibration curve at 480 nm, the drug release profile of DOX was analyzed.

1.6 ROS detection in vitro

The fluorescent probe 2',7'-Dichlorodihydrofluorescein (DCFH), obtained from 2',7'-dichlorodihydrofluorescein diacetate (DCFH-DA), was employed to assess the generation of reactive oxygen species (ROS). The aqueous solution of CDZ (4 mg/mL) was allowed to react completely with ATP (10 mM). Subsequently, DCFH (50 μM) was added into the solution. The resulting solutions were then exposed to irradiation using a 660 nm laser (0.8 W/cm^2) for 0-10 min, during which the variation in the fluorescence signal of the indicator was continuously monitored via a fluorescence spectrometer. The excitation wavelength was set at 488 nm, and the emission wavelength ranged from 500-700 nm. Both the excitation and emission slits were set at 5 nm.

1.7 Cell culture

HepG2 cells were purchased from Wuhan Proceed Life Technology Co., Ltd (China). HeLa cells (human cervix cancer cells) and 293 T cells (human renal epithelial cells were provided by the State Key Laboratory of Chemo/Biosensing and Chemometrics of Hunan

University (Changsha, China). The cell lines were cultured in Dulbecco's modified Eagle's medium (DMEM) supplemented with 10% fetal bovine serum (FBS) at 37 °C in a 5% CO_2 atmosphere. Subsequently, the cells were plated on a 35 mm confocal culture dish and incubated for 24 h to allow for cell attachment to the dish walls.

1.8 Cytotoxicity test

The cytotoxic effects of various treatments on cellular viability were assessed utilizing the CCK-8 assay, which quantifies mitochondrial activity in viable cells. This assay was conducted using commercial kits purchased from Beyotime (Nantong, China). Both 293T and HeLa cell lines were treated in four different ways.

CZ group: the cells were incubated with CZ (0, 20, 40, 60, 80, 100 μg/mL) for 48 h.

CZ + Laser group: after 48 h of incubation with CZ (0, 20, 40, 60, 80, 100 μg/mL), the cells were irradiated with a 660 nm laser (1.0 W/cm^2) for 5 min.

CDZ group: the cells were incubated with CDZ (0, 20, 40, 60, 80, 100 μg/mL) for 48 h.

CDZ + Laser group: after 48 h of incubation with CDZ (0, 20, 40, 60, 80, 100 μg/mL), the cells were irradiated with a 660 nm laser (1.0 W/cm^2) for 5 min.

1.9 Live and dead cell staining assay

The viability of cells after different treatments was quantitatively assessed using a Live/Dead Cell Staining Kit. The live/dead staining experiments were conducted in accordance with the manufacturer's instructions. Briefly, the HeLa cells (~ 5×10^4) were seeded into a cell culture dish and incubated for 24 h. The cells were randomly divided into six groups: (1) PBS group, (2) PBS + Laser group, (3) CZ group, (4) CZ + Laser group, (5) CDZ group, (6) CDZ + Laser group. For dead/live staining, the cells were incubated at 37 °C for 12 h. Subsequently, the DMEM medium was removed, and the cells were washed with PBS three times. Fresh DMEM medium was added to each dish, and the HeLa cells were exposed to laser irradiation for 5 min (660 nm, 1.0 W/cm^2). After irradiation, the

medium was removed carefully, and 1 μM Calcein acetoxymethyl ester (Calcein AM) and 1 μM Propidium iodide (PI) were added into each dish, followed by incubation for 30 min. After removal of the medium and three washes with PBS, all cell samples were imaged using a confocal laser scanning microscope (FV3000). λ_{ex} = 488 nm, λ_{em} = 500-550 nm for Calcein-AM; λ_{ex} = 560 nm, λ_{em} = 590-640 nm for PI.

CZ and CDZ final concentration: 80 μg/mL.

1.10 Fluorescence imaging of CDZ nanosystem in cells

For ATP-induced fluorescence imaging, HeLa cells were randomly divided into three groups: (1) untreated cells; (2) the cells incubated with CDZ (4 mg/mL) for 30 min; (3) the cells treated with apyrase (0.5 U/mL) for 30 min followed by incubation with CDZ (4 mg/mL) for 30 min.

To distinguish between normal cells (293T cells) and cancer cells (HepG2 and HeLa cells), both were incubated with CDZ (4 mg/mL) for 30 min.

Fluorescence images were obtained using a confocal fluorescence microscope (λ_{ex} = 640 nm, λ_{em} = 710-880 nm).

In colocalization fluorescence imaging, 4T1 cells were combined with Mito-Tracker Green (10 μM) (λ_{ex} = 488 nm; λ_{em} = 500-550 nm) and CDZ (4 mg/mL) (λ_{ex} = 640 nm; λ_{em} = 710-880 nm) for 30 min, and the fluorescence images of different channels were imaged separately using a confocal fluorescence microscope.

1.11 Cellular ROS detection

The intracellular ROS level was measured using 2,7-dichlorofluorescein diacetate (DCFH-DA). HeLa cells were cultured for 24 h, followed by replacement of the original medium with a fresh medium containing CDZ (4 mg/mL) and incubated for 30 min. Subsequently, HeLa cells were washed with PBS for 3 times and incubated with DCFH-DA (10 μM) for another 30 min. Finally, the cells were irradiated with a 660 nm laser (1.0

W/cm^2), and fluorescence imaging was performed using a Nikon confocal fluorescence microscope (λ_{ex} = 488 nm, λ_{em} = 500-600 nm).

1.12 Fluorescence imaging in mice

Female BALB/c nude mice (6-7 weeks old) were bought from Hunan Slike Jingda Laboratory Animal Co., Ltd. and were lovingly cared for throughout the experiment. All animal experiments were carried out according to the regulations issued by the Ethical Committee of Xiangtan University and approved by the Animal Ethics Committee of Hunan Slike Jingda Experimental Animal Co. LTD (SJA-ll-2023008).

The tumor-bearing mouse model was established by subcutaneously injection of 1×10^6 HeLa cells into the back of BALB/c nude mice, and the tumors were allowed to grow for 10 days before imaging.

To differentiate between normal mice and cancer mice, the normal mice and the tumor-bearing mice were intravenously injected with CDZ (10 mg/kg), respectively. After 1 h, the mice were anesthetized with continuous isofurane and imaged. After imaging, all the mice were sacrificed, and fluorescence imaging was performed on the main organs (heart, liver, spleen, lung, kidney) as well as the tumors.

Fluorescence imaging of mice and organs was acquired using a small animal optical system (λ_{ex} = 710 nm, λ_{em} = 750-850 nm).

1.13 Synergistic therapy evaluation in mice

Anti-tumor studies were conducted when the tumor volume reached 70 mm^3 (tumor volume = a$\times$b^2/2, a: maximum diameter, b: minimum diameter). The established HeLa tumor-bearing mice model was randomly divided into four groups (n = 3):

PBS group: the tumor-bearing mice were irradiated with a 660 nm laser after intravenous injection of saline on day 0, day 2, day 4, day 8, day 10 and day 12.

DZ group: the tumor-bearing mice were intravenously injected with DZ (10 mg/kg) on day 0, day 2, day 4, day 8, day 10 and day 12.

CZ group: the tumor-bearing mice were intravenously injected with CZ (10 mg/kg) and irradiated with a 660 nm laser for 10 min on day 0, day 2, day 4, day 8, day 10 and day 12.

CDZ group: the tumor-bearing mice were intravenously injected with CDZ (10 mg/kg) and irradiated with a 660 nm laser for 10 min on day 0, day 2, day 4, day 8, day 10 and day 12.

The photographs were taken on day 0, day 2, day 4, day 8, day 10, day 12 and day 14. The weight of mice and volumes of tumors were measured on day 0, day 2, day 4, day 8, day 10, day 12 and day 14. The relative tumor volumes were calculated as V/V_0 (V_0: the original tumor size, V: the tumor volume recorded during the phototherapy). The tumor volume was calculated as follows: volume = (tumor length) × (tumor width)^2/2. The relative body weights were calculated as M/M_0 (M_0: the original body weight, M: the body weight recorded during the phototherapy).

1.14 Histology analysis

The tissue samples, including the main organs (heart, liver, spleen, lung, kidney) as well as the tumors from different treatment groups on day 14, were fixed with 4% paraformaldehyde. They were then embedded in paraffin and sectioned to 4 μm for hematoxylin and eosin (H&E) staining.

1.15 Immune response

The serum proinflammatory cytokines IL-6 and TNF-α level in different groups of mice receiving different treatments were assessed by ELISA kits (Shanghai Enzyme-linked Biotechnology Co., Ltd.) following protocols recommended by the manufacturer. This analysis was performed on day 14 after different treatments.

1.16 Statistical analysis

Data were expressed as mean ± standard deviation. Student's t test was used to evaluate the statistical significance. P values < 0.05 were regarded statistically significant (*p < 0.05, **p < 0.01, ***p < 0.001, ****p < 0.0001).

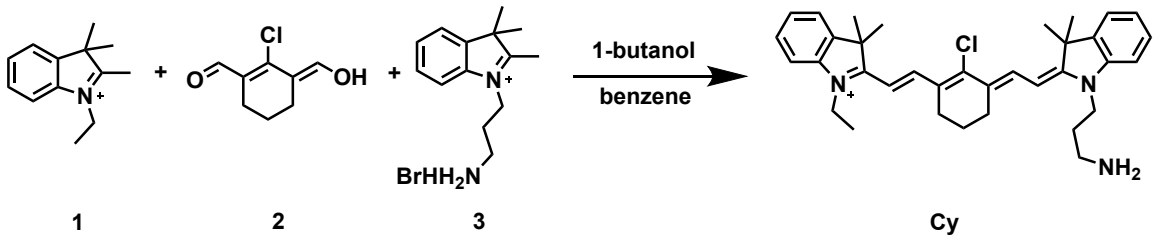

Scheme S1. Synthetic route of Cy.

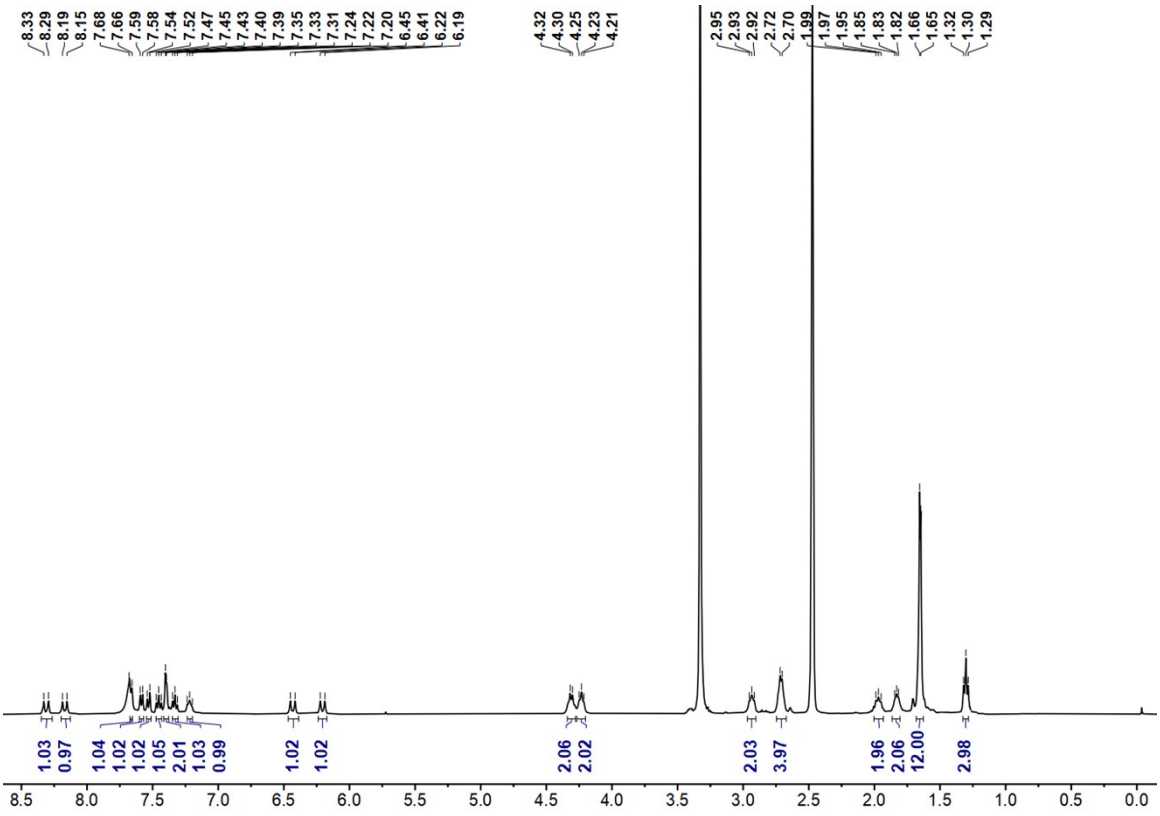

Fig. S1. ^{1}H NMR spectrum of compound Cy in DMSO-d_6.

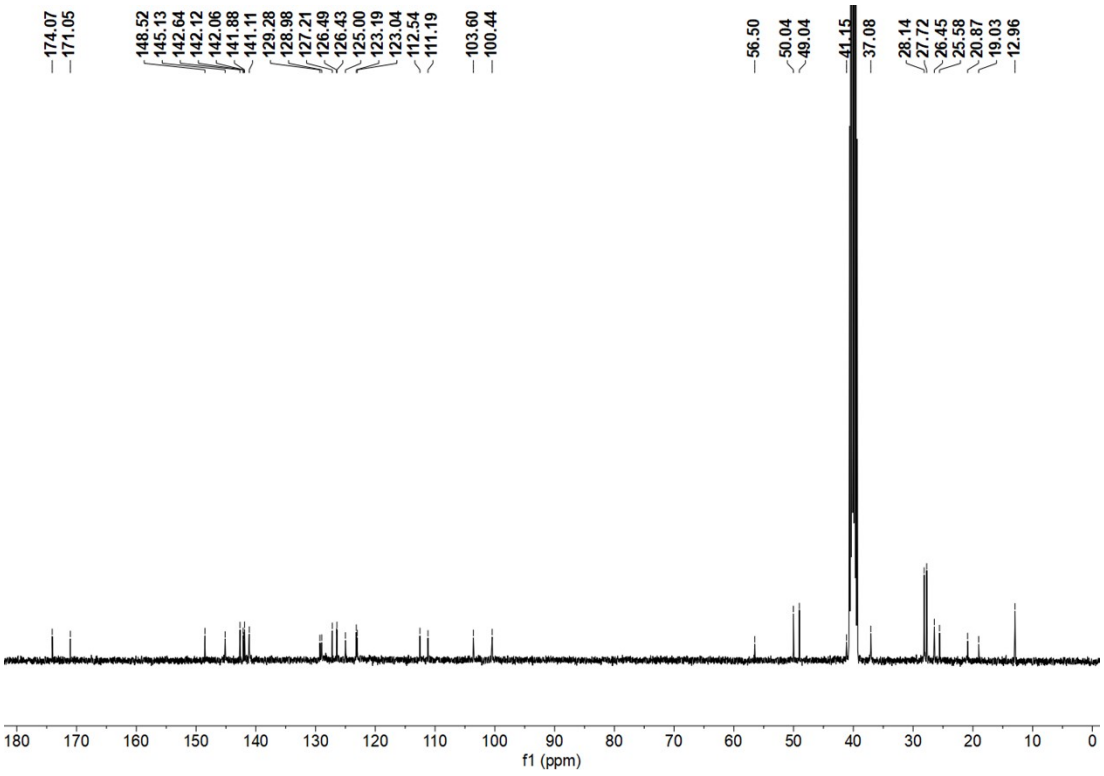

Fig. S2. ^{13}C NMR spectrum of compound Cy in DMSO-d_6.

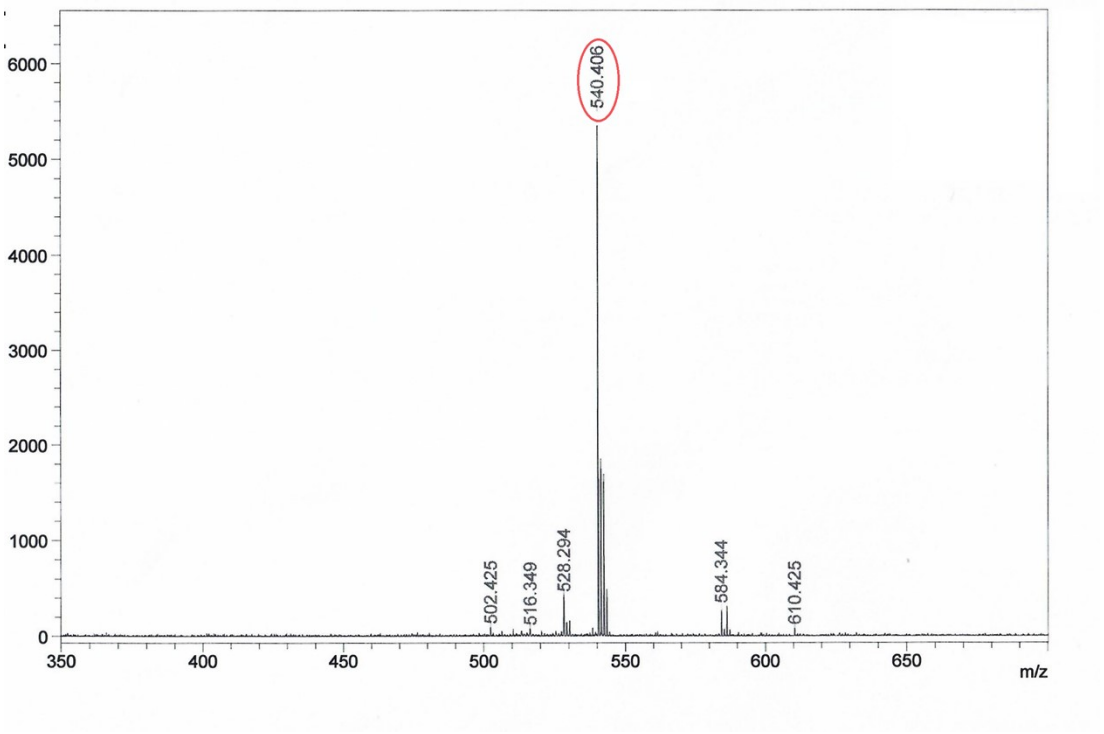

Fig. S3. MALDI-TOF mass spectrum of compound Cy.

Fig. S4. Photographs of ZIF-90, CZ and CDZ.

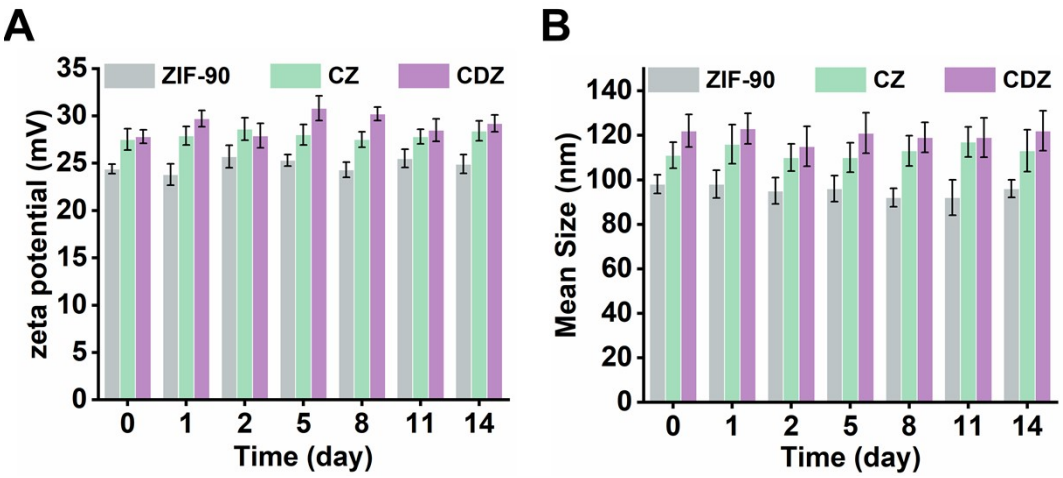

Fig. S5. Zeta potentials (A) and diameter (B) changes of ZIF-90, CZ, CDZ stored in PBS (pH 7.4) for two weeks, respectively. The date was obtained by three independent experiments (n = 3) and presented as mean ± SD.

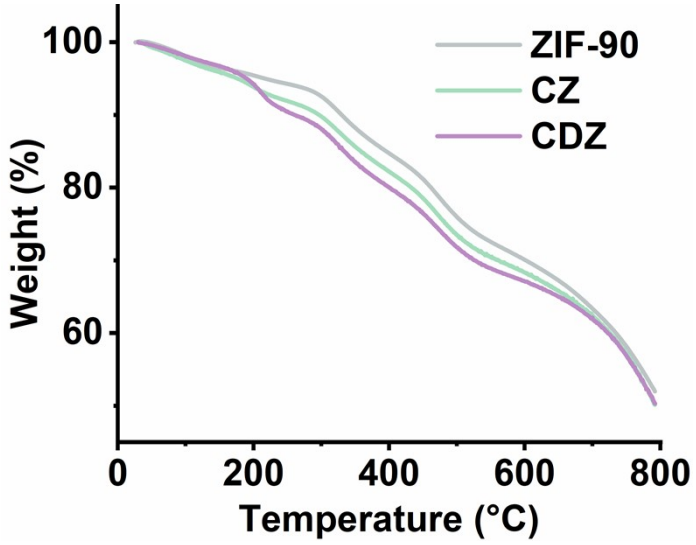

Fig. S6. Thermogravimetric analysis of ZIF-90, CZ, and CDZ.

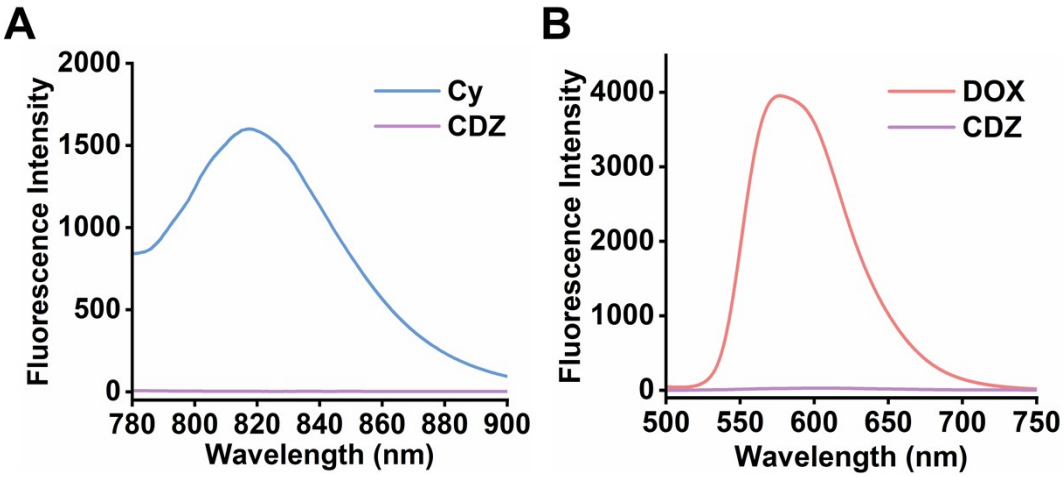

Fig. S7. Fluorescence spectra of A) Cy and CDZ, λ_{ex} = 770 nm; B) DOX and CDZ, λ_{ex} = 480 nm.

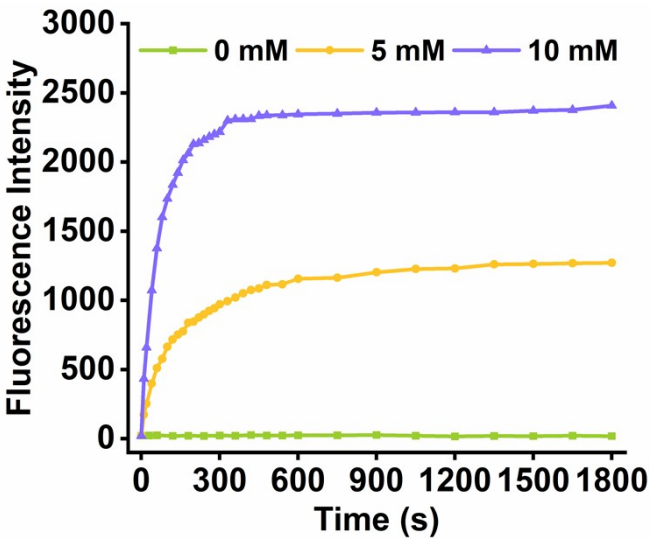

Fig. S8. Time-dependent fluorescence intensity of CDZ (4 mg/mL) upon the addition of ATP (0, 5, 10 mM) in HEPES buffer solution (pH 7.4, 10 mM, with 5% DMSO). $\lambda_{ex}/\lambda_{em}$ = 770/815 nm.

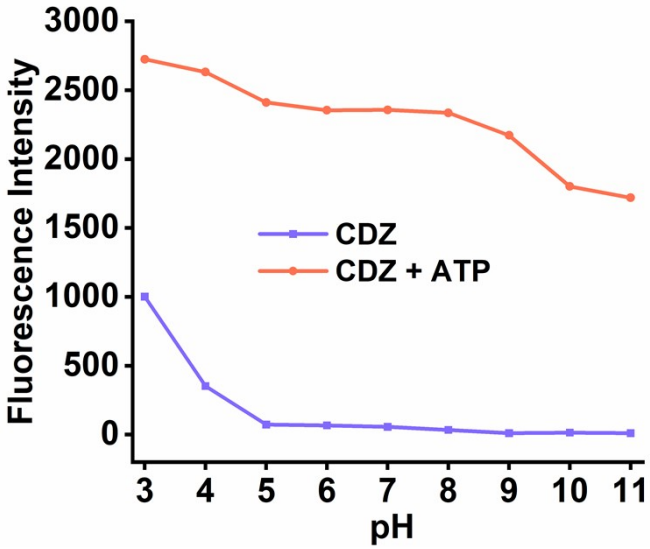

Fig. S9. Effect of pH on the fluorescence of CDZ (4 mg/mL) before and after reaction with ATP (10 mM). $\lambda_{ex}/\lambda_{em}$ = 770/815 nm.

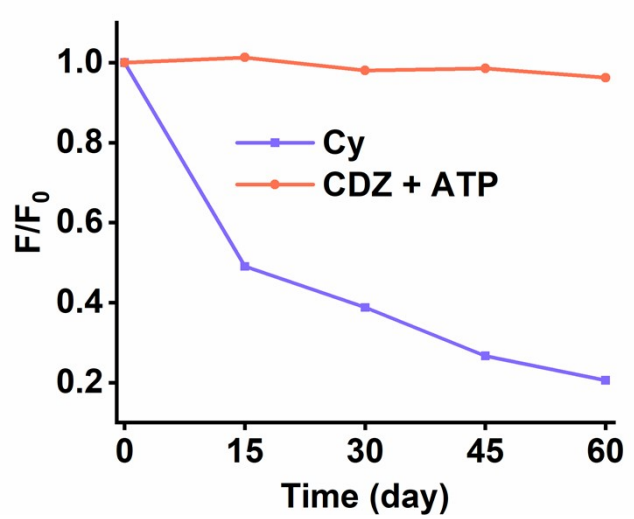

Fig. S10. Fluorescence intensities of CDZ (4 mg/mL) in response to ATP (10 mM) and Cy (10 μM) at different times stored at room temperature. $\lambda_{ex}/\lambda_{em}$ = 770/815 nm.

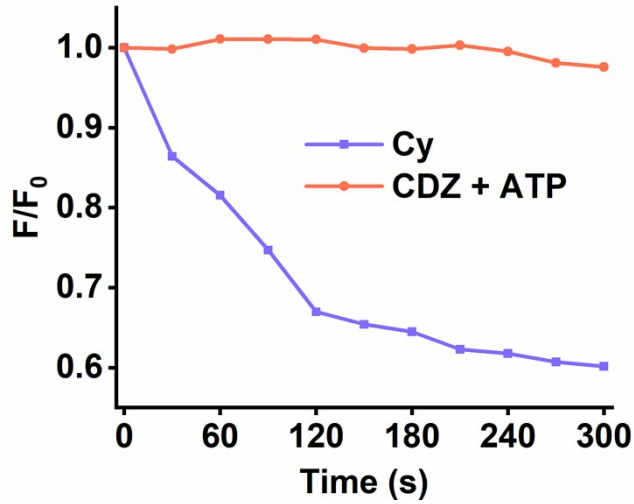

Fig. S11. Fluorescence intensity of Cy (10 μM) and CDZ (4 mg/mL) with ATP (10 mM) upon irradiation (660 nm, 0.8 W/cm^2). $\lambda_{ex}/\lambda_{em}$ = 770/815 nm.

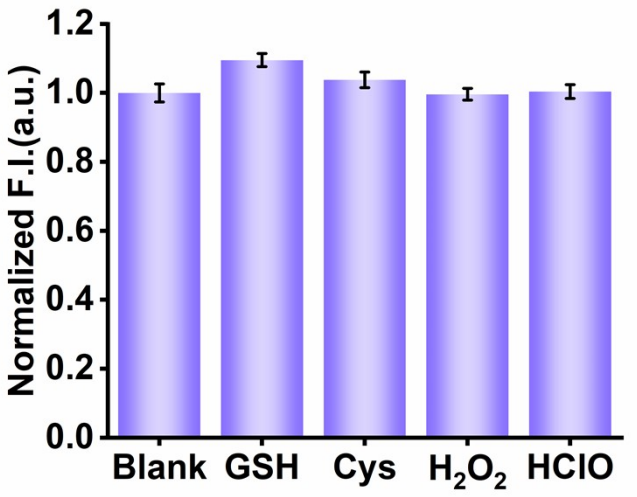

Fig. S12. Normalized fluorescence intensities of CDZ（4 mg/mL）treated with GSH (1 mM), Cys (1 mM), H_2O_2 (1 mM) and HClO (1 mM) for 60 min. The fluorescence intensities were normalized against the maximum value at 815 nm.

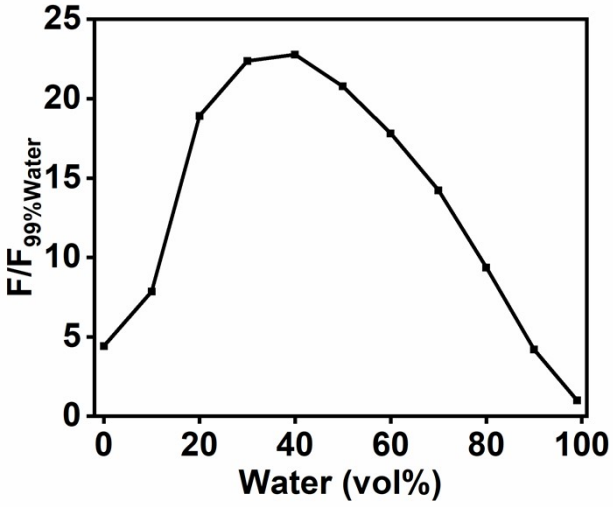

Fig. S13. Fluorescence intensity of Cy in DMSO/water mixtures with different fractions of water. $\lambda_{ex}/\lambda_{em}$ = 770/815 nm.

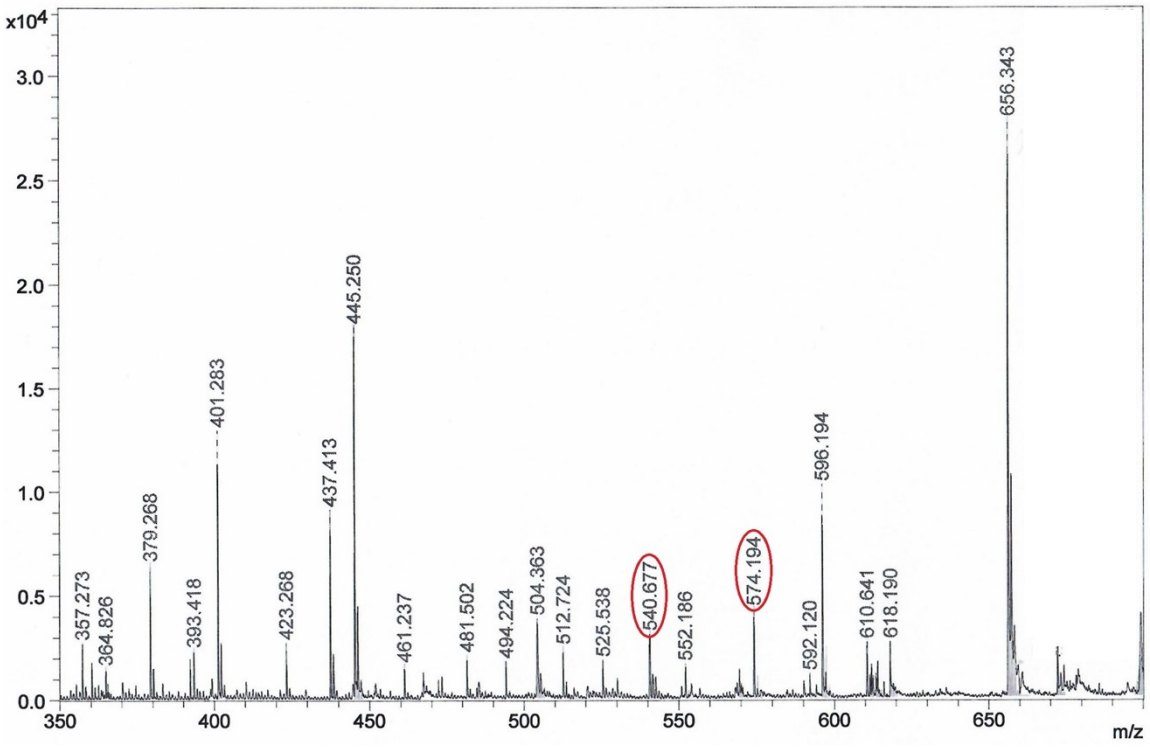

Fig. S14. MALDI-TOF mass spectra of CZ after reacting with ATP.

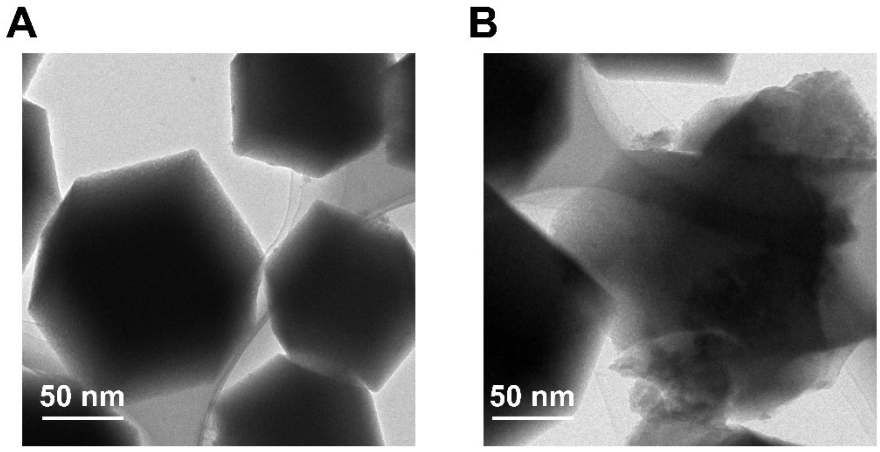

Fig. S15. TEM images of A) CDZ nanosystem and B) CDZ nanosystem reacted with ATP.

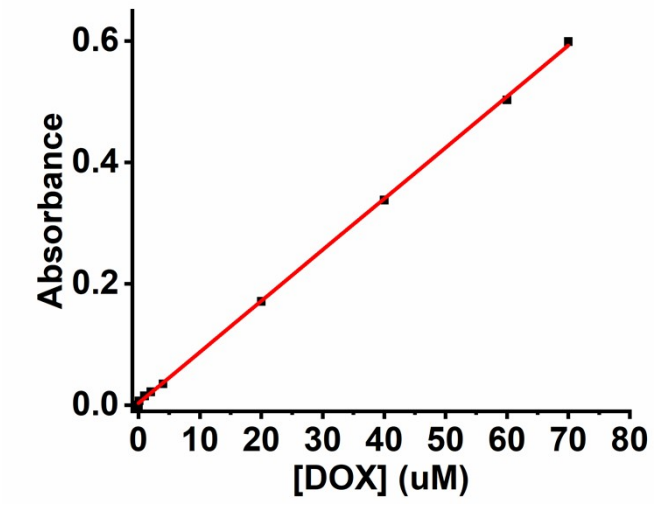

Fig. S16. The calibration curve of DOX at 480 nm.

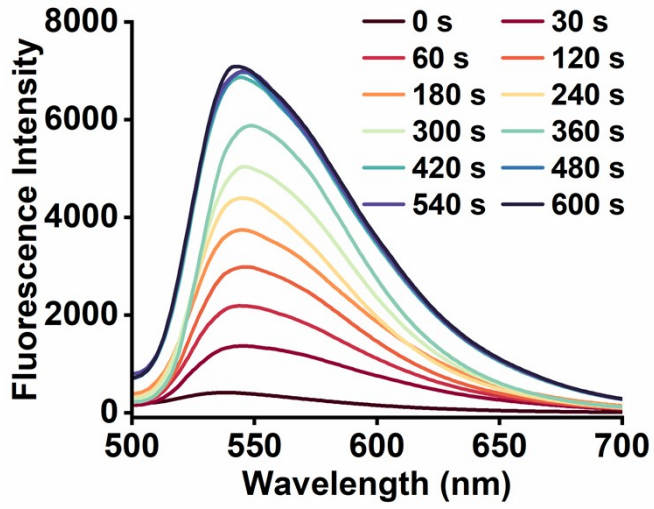

Fig. S17. The fluorescence spectra of DCFH (50 μM) incubated with CDZ (4 mg/mL) and ATP (10 mM) upon irradiation (660 nm, 0.8 W/cm^2). λ_{ex} = 488 nm.

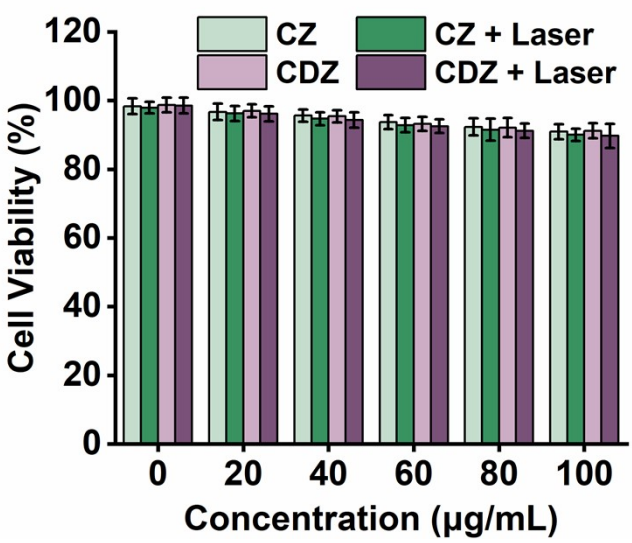

Fig. S18. Cell viabilities of 293T cells incubated with different concentrations (0, 20, 40, 60, 80 and 100 μg/mL) of the nanosystem CDZ by CCK-8 assay.

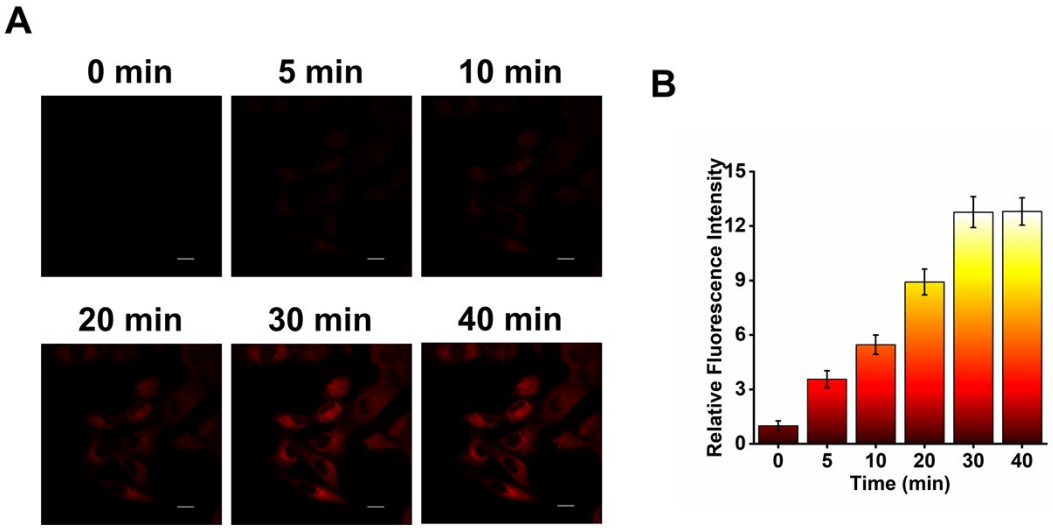

Fig. S19. A) The time-dependent fluorescence imaging of HeLa cells treated with CDZ nanoparticles (4 mg/mL). B) Relative fluorescence intensity of (A). λ_{ex} = 640 nm, λ_{em} = 710-880 nm. Scale bar: 20 μm.

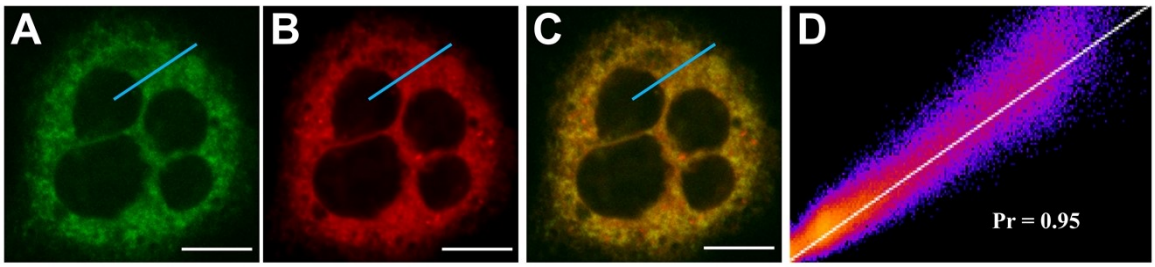

Fig. S20. Fluorescence images of 4T1 cells stained with (A) Mito-Tracker Green (10 μM) and (B) CDZ (4 mg/mL) for 30 min. (C) Merged image of images (A–B). (D) Fluorescence intensities for regions of interest (white line). Scale bar: 10 μm. For green channel: λ_{ex} = 488 nm； λ_{em} = 500-550 nm. For red channel: λ_{ex} = 640 nm, λ_{em} = 710-880 nm.

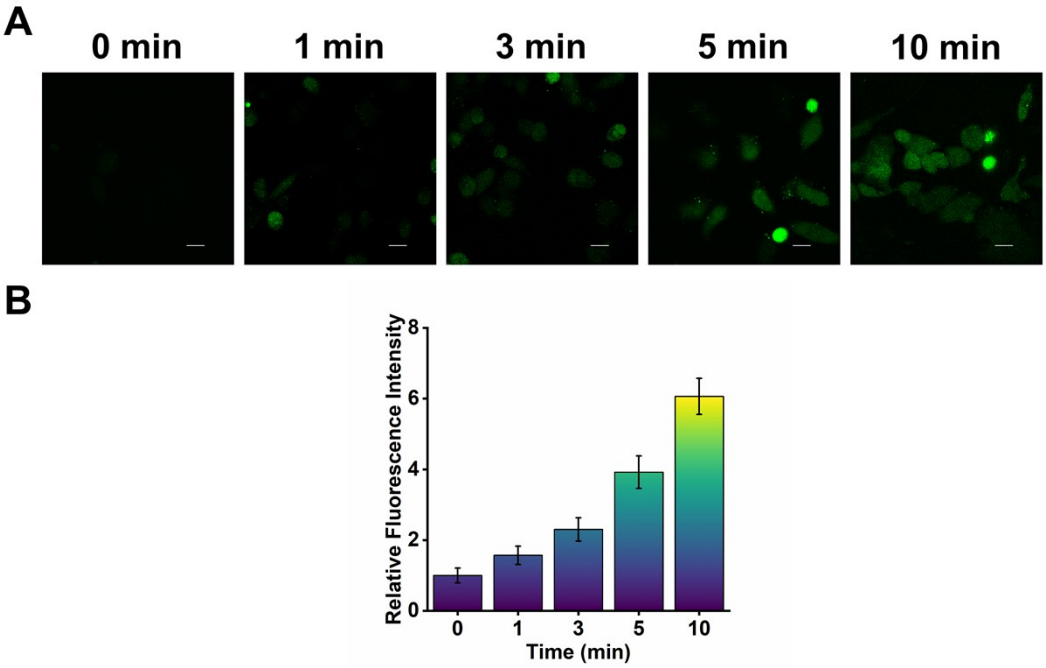

Fig. S21. A) Fluorescence imaging of HeLa cells incubated with CDZ (4 mg/mL) and DCFH-DA (10 μM) after laser irradiation for different times (0-10 min). B) Relative fluorescence intensity of (A). λ_{ex} = 488 nm, λ_{em} = 500-600 nm. Scale bar: 20 μm.

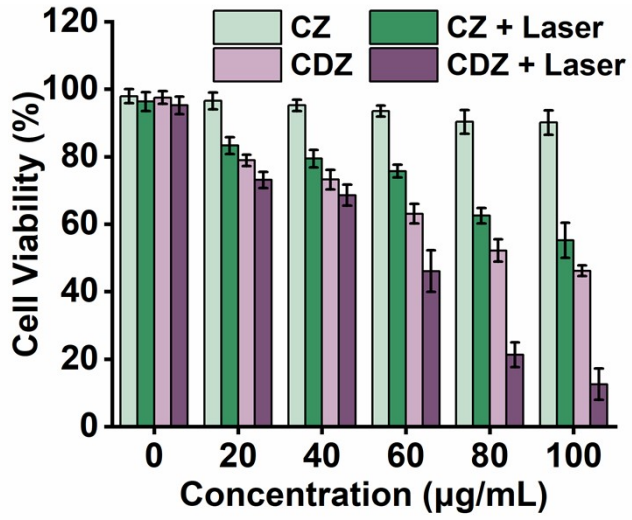

Fig. S22. Cell viabilities of HeLa cells incubated with different concentrations (0, 20, 40, 60, 80 and 100 μg/mL) of the nanosystem CDZ by CCK-8 assay.

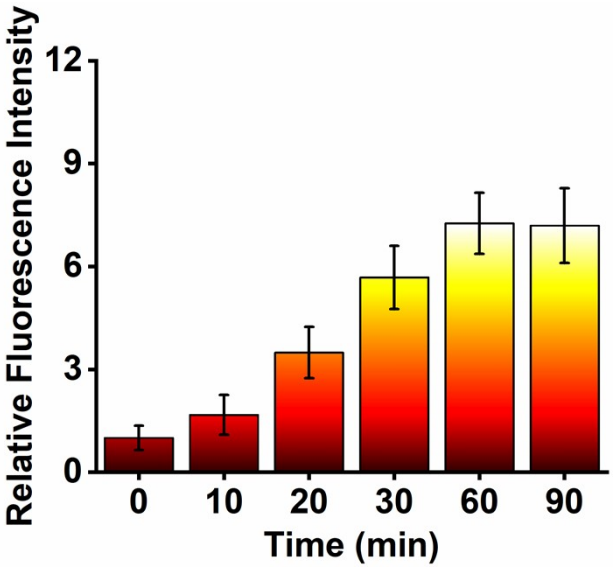

Fig. S23. Relative fluorescence intensity in Fig. 6D.

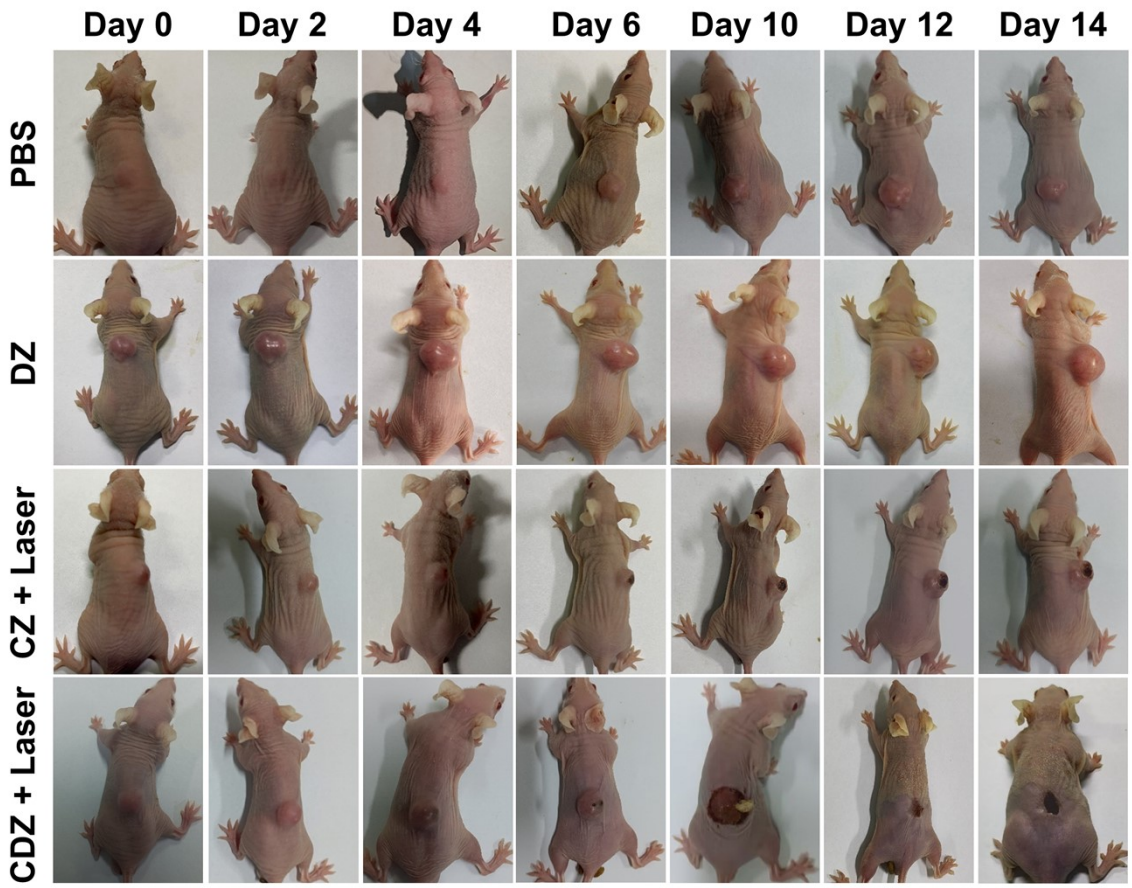

Fig. S24. Photographs of the HeLa tumor-bearing mice after different treatments.

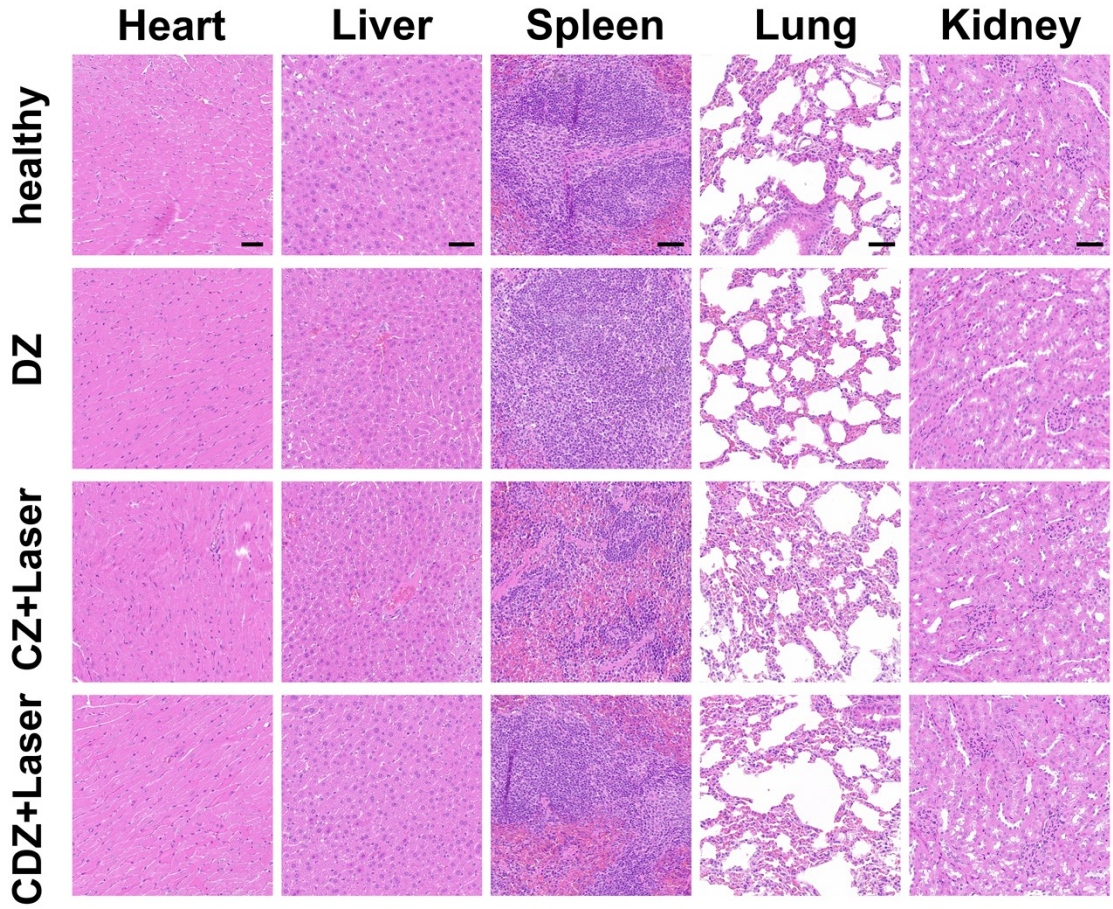

Fig. S25. H&E staining images of major organs (including heart, liver, spleen, lungs, and kidneys) excised from the healthy and tumor-bearing mice after treatment with different formulations on day 14. Scale bar: 50 μm.

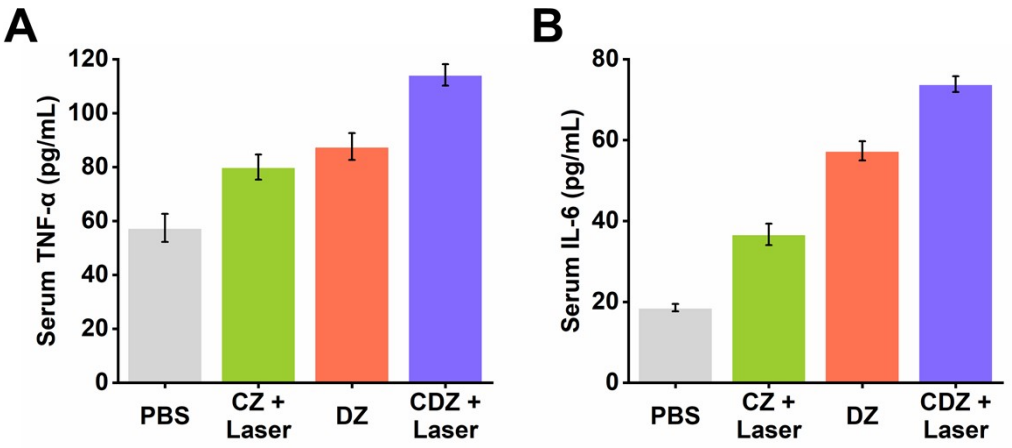

Fig. S26. The levels of A) TNF-α and B) IL-6 in serum of mice after different treatments on day 14.

References

[S1] Q. S. Gu, T. Li, W. X. Wang, Z. Q. Wang, Q. R. Liu, G. J. Mao, Y. F. Li and C. Y. Li, Sens. Actuators B Chem., 2023, 393, 134287.

[S2] M. J. Hou, Z. Q. Wang, J. T. Chen, Z. K. Tan, G. J. Mao, J. J. Fei and C. Y. Li, Anal. Chem., 2022, 94, 14257–14264.

[S3] X. X. Chen, M. J. Hou, W. X. Wang, M. Tan, Z. K. Tan, G. J. Mao, B. Yang, Y. F. Li and C. Y. Li, Nanoscale, 2022, 14, 3808–3817.